Russian Journal of Nonlinear Dynamics, 2021, vol. 17, no. 2, pp. 157–164.
Full-texts are available at http://nd.ics.org.ru
DOI: 10.20537/nd210202

MATHEMATICAL PROBLEMS OF NONLINEARITY

MSC 2010: 37G10, 37G35

On the Organization of Homoclinic Bifurcation Curves in Systems with Shilnikov Spiral Attractors

Y. V. Bakhanova, A. A. Bobrovsky, T. K. Burdygina, S. M. Malykh

We study spiral chaos in the classical Rössler and Arneodo – Coullet – Tresser systems. Special attention is paid to the analysis of bifurcation curves that correspond to the appearance of Shilnikov homoclinic loop of saddle-focus equilibrium states and, as a result, spiral chaos. To visualize the results, we use numerical methods for constructing charts of the maximal Lyapunov exponent and bifurcation diagrams obtained using the MatCont package.

Keywords: Shilnikov bifurcation, spiral chaos, Lyapunov analysis

Received May 20, 2021
Accepted June 09, 2021

This paper was supported by the Laboratory of Dynamical Systems and Applications NRU HSE, of the Ministry of Science and Higher Education of the RF grant No. 075-15-2019-1931. Numerical results presented in Section 2 were obtained by the RSF grant 19-71-10048.

Yuliya V. Bakhanova
bakhanovayu@gmail.com
Andrey A. Bobrovsky
piqzo1999@mail.ru
Tatiana K. Burdygina
tatjana.burdygina@gmail.com
Semyon M. Malykh
malykhsm@gmail.com
National Research University "Higher School of Economics"
ul. Bolshaya Pecherskaya 25/12, Nizhny Novgorod, 603155 Russia

1. Introduction

In this paper we present some results of studying the organization of homoclinic bifurcation curves in the Rössler [1] and Arneodo – Coullet – Tresser [2] models. These are two well-known classical systems that demonstrate chaotic attractors caused by the presence of Shilnikov saddle-focus [3]. First, we consider the Rössler system given by the following equations:

$$\begin{cases} \dot{x} = -y - z, \\ \dot{y} = x + ay, \\ \dot{z} = bx - z(c - x). \end{cases} \tag{1.1}$$

Here x, y, z are system variables, a, b and c are positive parameters, for our study we have fixed the parameter $b = 0.3$. There exist several similar representations for the Rössler model, see also [4]. The representation above is chosen due to the fact that the equilibrium state O_1 is always located at the point $(0, 0, 0)$ and does not depend on any parameter of the system. It is convenient to use this feature in numerical experiments. The second equilibrium state O_2 has the coordinates $(c - ab, b - c/a, -(b - c/a))$. For the Rössler system the applicability of the famous Shilnikov theorem on the existence of chaotic dynamics near a loop of saddle-focus was first shown in [2]. A detailed two-parameter analysis near the homoclinic bifurcation curve in this system was carried out in [5]. Note that system (1.1) is a strongly dissipative system with slow x, y and fast z variables due to strongly negative divergence.

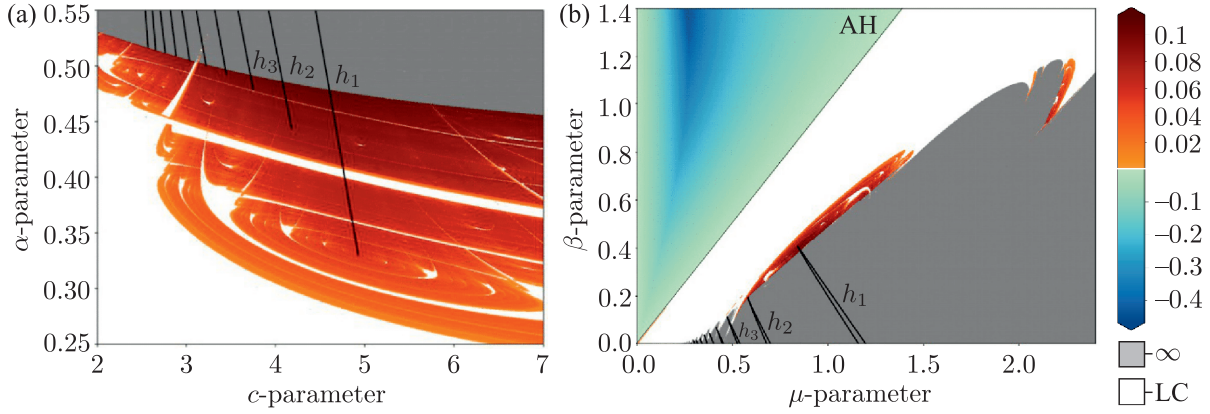

Fig. 1. Charts of the maximal Lyapunov exponent superimposed with homoclinic bifurcation curves $h_1, h_2, \ldots$ for the Rössler model (1.1) (panel (a)) and for the Arneodo – Coullet – Tresser model (1.2) (panel (b)). Gray indicates the region with trajectories going to infinity, the region of the chaotic attractor existence is shown by red-orange colors, white regions correspond to stable periodic orbits. Homoclinic curves are colored in black.

Figure 1 shows a chart of the maximal Lyapunov exponent superimposed with homoclinic bifurcation curves for the systems under study. It is clearly seen that chaotic regions alternate with stability windows. Such a structure of Lyapunov diagrams is typical for systems with quasi-attractors [6]. In particular, for systems with a Shilnikov homoclinic loop, the structure of stability windows was described in [5], see also [7]. Note that the black curves $h_1, h_2, \ldots$ presented in Fig. 1a correspond to a Shilnikov homoclinic bifurcation with equilibrium O_1. From [8, 9] it is known that such homoclinic curves have a parabola-like (U-shape) form. We have found these homoclinic curves and placed them over the charts of the maximal Lyapunov exponent for clarity.

The second model under consideration was introduced by Arneodo, Coullet and Tresser in [2]. It has the following form:

$$\begin{cases} \dot{x} = y, \\ \dot{y} = z, \\ \dot{z} = -y - \beta z + \mu x(1 - x). \end{cases} \tag{1.2}$$

As in the model (1.1), here x, y, z are variables, while β and μ are parameters. There are two equilibrium states O_1 $(1, 0, 0)$ and O_2 $(0, 0, 0)$ in this system. The stability of these equilibrium states depends on values of parameters β and μ. They can be stable or completely unstable. Also note that these equilibria can undergo an Andronov – Hopf bifurcation. Figure 1b shows the chart of the maximal Lyapunov exponent and homoclinic bifurcation curves h_1, h_2, h_3 for system (1.2). One can note that this diagram is similar to the analogous diagram for the model (1.1) (cf. Figs. 1a and 1b).

The line that separates the region with a stable limit cycle from the region with the stable equilibrium O_1 can be seen in Fig. 1b. This line corresponds to the supercritical Andronov – Hopf bifurcation. Below this line O_1 changes its type and becomes a saddle-focus equilibrium with 1D stable and 2D unstable manifolds. Note that the divergence of the system is constant and equal to $-\beta$, so attractors can exist only in the case $\beta > 0$, while for $\beta < 0$ system (1.2) can have repellers which can even be chaotic. Further, we show that all attractors in this system are associated with equilibrium O_1, while repellers appear due to equilibrium O_2.

This work is devoted to the study of the global behavior of homoclinic bifurcation curves $h_1, h_2, \ldots$ in two systems under consideration. Using MatCont software we demonstrate that these curves are pieces of the same bifurcation curve, and each of its U-shaped pieces, which we call h_i, corresponds to an i-round homoclinic loop. In addition, we explain why there are no other homoclinic bifurcation curves between the thin U-shaped pieces of this curve, but there are complex sets of secondary bifurcation curves inside each such piece. Using the Arneodo – Coullet – Tresser model (1.2) as an example, we study the structure of these loops in detail.

The paper is organized as follows: first, a one-parameter bifurcation analysis is carried out for the model (1.2) in Section 2. Section 3 shows the results of a two-parameter bifurcation analysis and describes the construction of multi-round homoclinic curves.

2. One-parameter bifurcation analysis.

There is a well-known fact, repeatedly proven for both the Arneodo – Coullet – Tresser model and the Rössler model (see, e.g., [10, 11]), that chaos in these systems is developed via the Shilnikov scenario [12] from the stable equilibrium. Let us demonstrate it using system (1.2) as an example.

First, we fix $\beta = 0.4$ and increase parameter μ. When $0 < \mu < \mu_1 = 0.4$, the equilibrium state O_1 is the only attractor in the system. When $\mu > \mu_1$, the equilibrium state O_1 loses stability through a supercritical Andronov – Hopf bifurcation and becomes a saddle-focus, and a stable limit cycle appears near it. The stable limit cycle exists on the interval $\mu_1 < \mu < \mu_2 \approx 0.72$ (see Fig. 2a). Starting from $\mu = \mu_2$, the limit cycle undergoes a cascade of period-doubling bifurcations (see Figs. 2b, 2c, 2d, where 2-, 4- and 8- periodic cycles are shown) that leads to a strange attractor of Hénon type (if one considers bifurcations on a corresponding Poincaré map), see Fig. 2e. With a further increase of μ up to $\mu_3 \approx 0.86311445$, attractor trajectories start to pass arbitrarily close to the saddle-focus O_1, a homoclinic loop appears and we consider

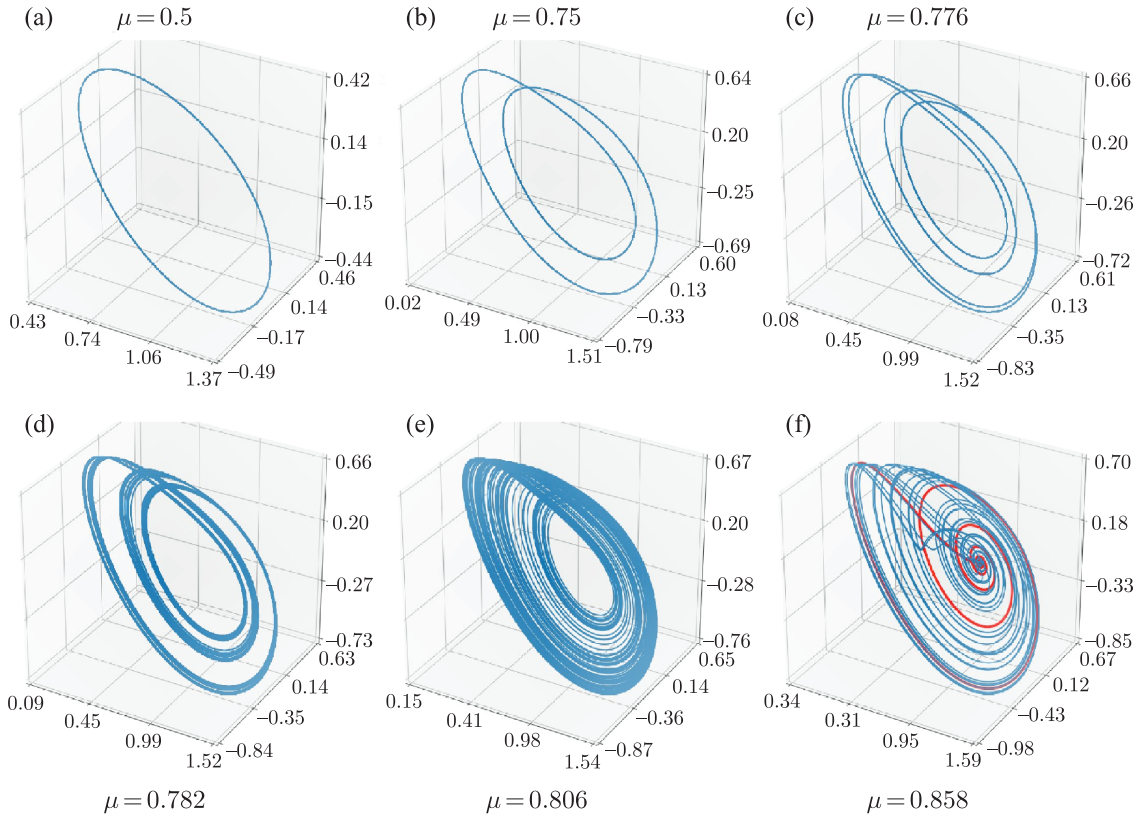

Fig. 2. One-parameter bifurcation analysis in the Arneodo – Coullet – Tresser model (1.2): from the stable equilibrium to the Shilnikov attractor containing the saddle-focus O_1 with the 2D unstable invariant manifold.

this to be the moment of creation of a Shilnikov spiral attractor, see Fig. 2f, which shows the attractor with its primary homoclinic loop marked in red.

It is important to note that arbitrarily small changes of parameters split this homoclinic orbit. However, in its small neighborhood there exist double, triple and other multi-round homoclinic orbits [9, 13]. In order to illustrate it, let us provide the following numerical experiment based on the fact that, when a homoclinic loop exists, the saddle-focus equilibrium becomes part of an attractor, i.e., orbits in the attractor pass arbitrarily close to this equilibrium. Following [10, 14], we compute a distance between a sufficiently long orbit in the attractor and the saddle-focus equilibrium. If this distance is less than some small threshold, we assume that a homoclinic orbit exists. Then we compute a graph of minimal distance between the attractor and the saddle-focus. Each minimum approaching zero corresponds to a homoclinic orbit. Figure 3 shows the corresponding graph of minimal distance for system (1.2) for a fixed value of $\beta = 0.02$. Homoclinic orbits for each of its four minima superimposed with the corresponding attractor are shown in Figs. 4a–4d.

The same scenario is observed in the Rössler system (1.1) (see, e.g., [10, 11]).

From Fig. 1 it can be seen that several homoclinic curves enter the region with chaos, the structure and shape of the attractors on these curves are different and become more and more complex with decreasing parameter c in the Rössler model (1.1) and μ in the Arneodo – Coullet – Tresser model (1.2). So, the aim of this work is to study the structure of homoclinic bifurcation curves in two systems under consideration.

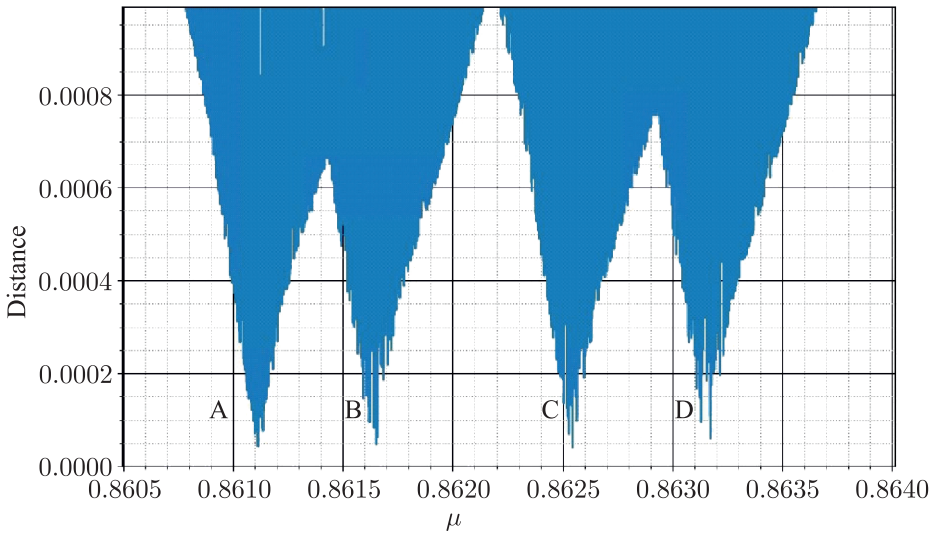

Fig. 3. The diagram of the minimum distances from the attractor to the saddle-focus equilibrium state $(1, 2)$ at $\beta = 0.02$, $0.8605 \leqslant \mu \leqslant 0.864$ for the Arneodo – Coullet – Tresser model (1.2).

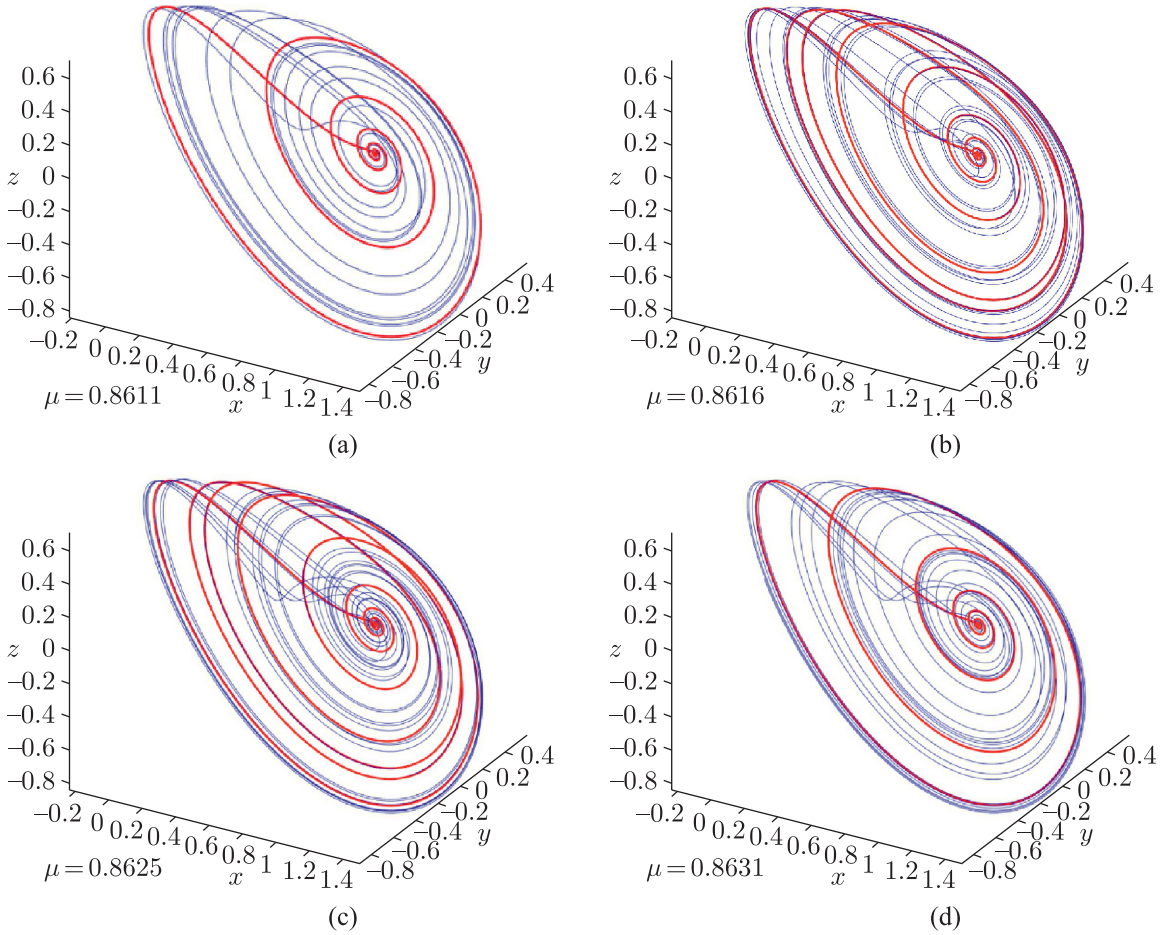

Fig. 4. Four different Shilnikov attractors corresponding to the four minima in the distance graph presented in Fig. 3. Homoclinic loops are colored in red.

In the next section we explain the arrangement of homoclinic bifurcation curves corresponding to the presented homoclinic orbits on the parameter plane (μ, β) using the Arneodo – Coullet – Tresser model as a case of study.

3. Two-parameter bifurcation analysis.

In this section we present two main results of two-parameter bifurcation analysis for systems (1.1) and (1.2). The first result is that homoclinic bifurcation curves $h_1, h_2, \ldots$ are pieces of one curve that looks like a "saw" with several "teeth" for both models under consideration. To show this, we take the homoclinic bifurcation curve h_1 from Fig. 1, which corresponds to the simplest homoclinic loop, and continue it on the corresponding parameter planes using MatCont software. To do it we choose the initial condition for the algorithm work using diagrams of the minimum distance. The resulting homoclinic bifurcation curves superimposed with the Lyapunov diagrams for systems (1.1) and (1.2) are shown in Fig. 5a and 5b, respectively. From these figures one can see that the continuation of h_1 indeed gives the long "saw"-like curve whose other "teeth" coincide with the curves $h_2, h_3, \ldots$. We call this curve a *primary homoclinic curve*.

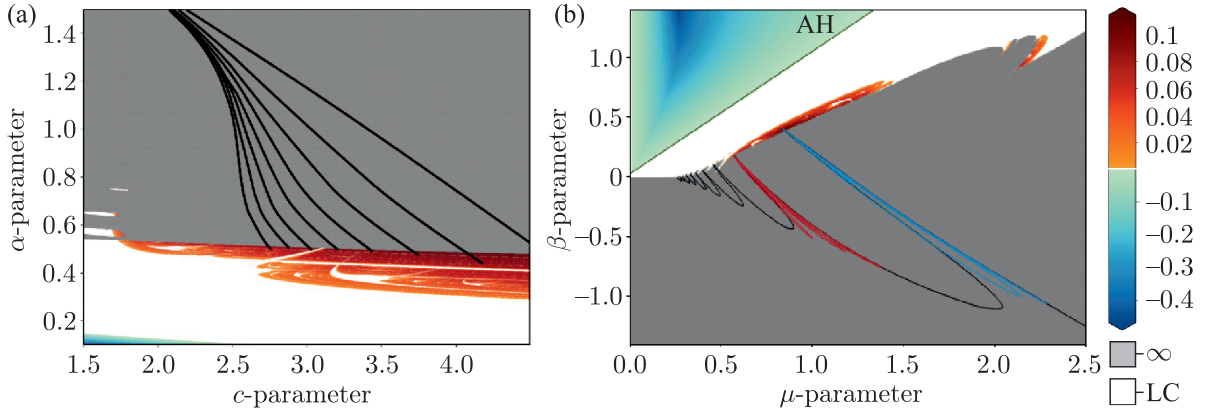

Fig. 5. Charts of the maximal Lyapunov exponent superimposed with homoclinic curves for the Rössler model (panel (a)) and for the Arneodo – Coullet – Tresser model (panel (b)). The black curves on both charts are primary homoclinic curves, the blue and red ones on panel (b) are secondary homoclinic curves.

The second important result is that there are no other homoclinic bifurcation curves between teeth $h_1, h_2, \ldots$, because of the splitting homoclinic loop "outside", which prevents the formation of secondary loops. The graphs of the distance between the saddle-focus and the attractor confirm it, i.e., the distance does not vanish in the regions between the teeth (see [10] for system (1.1)), which means that the saddle-focus does not belong to the attractor and there is no homoclinic loop in the system for these values of parameters.

On the other hand, according to the diagram of the minimum distance presented in Fig. 3 for system (1.2), between the two branches of h_1, which we call h_1^l and h_1^r, the distance is very close to zero at some points. It gives numerical evidence of the appearance of other homoclinic loops. We call such loops *secondary homoclinic loops*. The result of continuation of such loops below the teeth h_1 and h_2 for system (1.2) are shown in blue and red in Fig. 5b, respectively. Note that the blue bifurcation curve corresponds to a double homoclinic loop, while the red curve corresponds to the triple homoclinic loop.

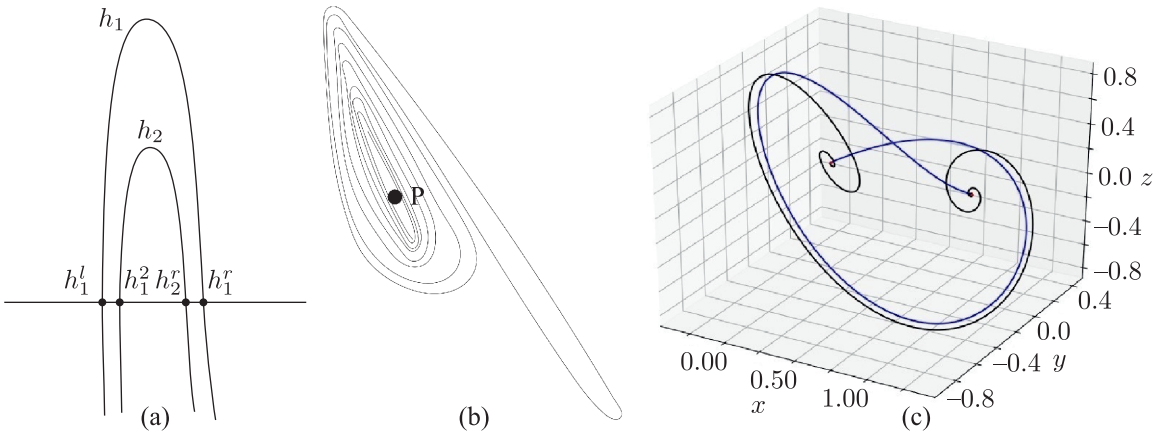

Fig. 6. (a) Schematic representation of the enlarged part of the primary homoclinic curve. (b) Schematic representation of an enlarged portion of the secondary homoclinic curve. (c) Bykov-like heteroclinic cycle for the Arneodo – Coullet – Tresser model (1.2).

The fact that we found these curves confirms that below each such tooth of the primary homoclinic bifurcation curve there is a set of secondary homoclinic bifurcation curves. It is schematically represented in Fig. 6a. Note that this sketch of the bifurcation diagram is in full agreement with what we get in the numerically obtained diagram of the minimum distance. It is clearly seen that points A, B, C, D in Fig. 3 correspond to points h_1^l, h_2^l, h_2^r, h_1^r.

Finally, we note that the secondary homoclinic bifurcation curves round onto the codimension-two points that correspond to the Bykov-like heteroclinic cycles [15]. We illustrate it by the secondary homoclinic bifurcation curves existing below h_1 and h_2, see the corresponding bifurcation sketch in Fig. 6b. The simplest heteroclinic cycle connecting two saddle-foci O_1 and O_2 is shown in Fig. 6c.

4. Conclusion

We have provided a detailed one- and two-parameter bifurcation analysis for the Arneodo – Coullet – Tresser model (1.2). This model was chosen because it is easier to study than the Rössler model (1.1) with strong dissipation in the system. We also showed that there is only one primary bifurcation homoclinic curve in the system that looks like a "saw" with several "teeth" in the bifurcation diagram. The existence of secondary homoclinic bifurcation curves was established below the primary one. The shape of secondary homoclinic bifurcation curves gave us the idea to search for Bykov heteroclinic cycles in the system, the simplest of which we found and presented in Fig. 6c. We believe that these results are relevant also for the Rössler model (1.1), including the organization of secondary homoclinic bifurcation curves. We will show it in our future work.

The authors thank A. Kazakov for the problem statement and fruitful discussions.

References

[1] Rössler, O. E., An Equation for Continuous Chaos, *Phys. Lett. A,* 1976, vol. 57, no. 5, pp. 397–398.

[2] Arnéodo, A., Coullet, P., and Tresser, C., Oscillators with Chaotic Behavior: An Illustration of a Theorem by Shil'nikov, *J. Statist. Phys.,* 1982, vol. 27, no. 1, pp. 171–182.

[3] Shilnikov, L. P., A Case of the Existence of a Denumerable Set of Periodic Motions, *Soviet Math. Dokl.,* 1965, vol. 6, pp. 163–166; see also: *Dokl. Akad. Nauk SSSR,* 1965, vol. 160, pp. 558–561.

[4] Rössler, O. E., Continuous Chaos: Four Prototype Equations, *Ann. New York Acad. Sci.,* 1979, vol. 316, no. 1, pp. 376–392.

[5] Gaspard, P., Kapral, R., and Nicolis, G., Bifurcation Phenomena Near Homoclinic Systems: A Two-Parameter Analysis, *J. Statist. Phys.,* 1984, vol. 35, nos. 5–6, pp. 697–727.

[6] Afraimovich, V. S. and Shil'nikov, L. P., Strange Attractors and Quasiattractors, in *Nonlinear Dynamics and Turbulence,* G. I. Barenblatt, G. Iooss, D. D. Joseph (Eds.), Interaction Mech. Math. Ser., Boston, Mass.: Pitman, 1983, pp. 1–34.

[7] Barrio, R., Blesa, F., Serrano, S., and Shilnikov, A., Global Organization of Spiral Structures in Biparameter Space of Dissipative Systems with Shilnikov Saddle-Foci, *Phys. Rev. E,* 2011, vol. 84, no. 3, 035201, 5 pp.

[8] Vitolo, R., Glendinning, P., and Gallas, J. A., Global Structure of Periodicity Hubs in Lyapunov Phase Diagrams of Dissipative Flows, *Phys. Rev. E,* 2011, vol. 84, no. 1, 016216, 7 pp.

[9] Gonchenko, S. V., Turaev, D. V., Gaspard, P., and Nicolis, G., Complexity in the Bifurcation Structure of Homoclinic Loops to a Saddle-Focus, *Nonlinearity,* 1997, vol. 10, no. 2, pp. 409–423.

[10] Malykh, S., Bakhanova, Yu., Kazakov, A., Pusuluri, K., and Shilnikov, A., Homoclinic Chaos in the Rössler Model, *Chaos,* 2020, vol. 30, no. 11, 113126, 18 pp.

[11] Gonchenko, A. S., Gonchenko, S. V., Kazakov, A. O., Kozlov, A. D., and Bakhanova, Yu. V., Mathematical Theory of Dynamical Chaos and Its Applications: Review. Part 2. Spiral Chaos of Three-Dimensional Flows, *Izv. Vyssh. Uchebn. Zaved. Prikl. Nelin. Dinam.,* 2019, vol. 27, no. 5, pp. 7–52 (Russian).

[12] Shilnikov, L. P., Bifurcation Theory and Turbulence, in *Methods of the Qualitative Theory of Differential Equations,* E. A. Leontovich (Ed.), Gorky: GGU, 1986, pp. 150–163 (Russian).

[13] Gaspard, P., Generation of a Countable Set of Homoclinic Flows through Bifurcation, *Phys. Lett. A,* 1983, vol. 97, nos. 1–2, pp. 1–4.

[14] Bakhanova, Yu. V., Kazakov, A. O., Korotkov, A. G., Levanova, T. A., and Osipov, G. V., Spiral Attractors As the Root of a New Type of "Bursting Activity" in the Rosenzweig – MacArthur Model, *Eur. Phys. J. Spec. Top,* 2018, vol. 227, nos. 7–9, pp. 959–970.

[15] Bykov, V. V., Orbit Structure in a Neighborhood of a Separatrix Cycle Containing Two Saddle-Foci, in *Methods of Qualitative Theory of Differential Equations and Related Topics,* Amer. Math. Soc. Transl. Ser. 2, vol. 200, Adv. Math. Sci., vol. 48, Providence, R.I.: AMS, 2000, pp. 87–97.